

## Model-based characterisation of twin-screw granulation system for continuous solid dosage manufacturing

Ashish Kumar<sup>a,b</sup>, Krist V. Gernaey<sup>c</sup>, Thomas De Beer<sup>d</sup> and Ingmar Nopens<sup>b,\*</sup>

<sup>a</sup>BIOMATH, Dept. of Mathematical Modelling, Statistics and Bioinformatics, Faculty of Bioscience Engineering, Ghent University, Coupure Links 653, B-9000 Gent, Belgium

<sup>b</sup>Laboratory of Pharmaceutical Process Analytical Technology, Dept. of Pharmaceutical Analysis, Faculty of Pharmaceutical Sciences, Ghent University, Harelbekestraat 72, B-9000 Ghent, Belgium

<sup>c</sup>CAPTEC-PROCESS, Department of Chemical and Biochemical Engineering, Technical University of Denmark, 2800 Kongens Lyngby, Denmark

\*Ingmar.Nopens@UGent.be

### Abstract

Continuous twin-screw granulation has received increased attention as it can be embedded in a continuous manufacturing line allowing 24/7 production capacity eliminating scale-up requirements and intermediate storage. The screws have a modular structure (interchangeable transport and kneading discs) allowing greater flexibility in equipment design. However, process knowledge should be further developed both under steady state and dynamic conditions. Mechanistic models incorporating the underlying mechanisms are therefore applied. In this study, the principle constitutive mechanisms such as aggregation and breakage are included in a population balance modelling framework. Based on an experimental inflow granule size distribution and mean residence time of the granulator, predictions of the outflow granule size distribution were made. Experimental data was used for calibrating the model for individual screw modules in the twin-screw granulator. The results showed that the successive kneading blocks lead to a granulation regime-separation inside the twin-screw granulator. The first kneading block after wetting caused an increase in the aggregation rate, which was reduced after the second kneading block. The breakage rate increased successively along the length of the granulator. Such a physical separation between the granulation regimes will be promising for future design and advanced control of the continuous granulation process.

**Keywords:** continuous manufacturing, population balance modelling, wet granulation.

### 1. Introduction

Continuous manufacturing of pharmaceutical solid dosage forms has received great interest in the last decade due to several process and economic benefits associated with it. A continuous process with 24/7 production capacity will eliminate scale-up requirements and intermediate storage. With this in mind, twin-screw granulation has emerged as promising method for particle size enlargement to achieve better flow properties and avoid segregation during successive unit operations. A twin-screw granulator (TSG) can be embedded in a continuous manufacturing line which also includes dryer, screening unit and tableting machine making continuous powder to tablet production

possible. Moreover, the screws used in the granulator have a modular structure (interchangeable transport and kneading discs) providing flexibility towards adaptation in equipment and process variables depending upon on feed characteristics to achieve the required product characteristics. The available studies have primarily focused on the effect of process variables (such as screw configuration, material throughput, screw speed etc.) (Vercruysse et al., 2012; Dhenge et al., 2011; Thompson and Sun, 2010) and formulation properties (El Hagrasy et al., 2013; Dhenge et al., 2013) on granule properties at the outlet of the TSG due to the opacity of the multiphase system. Thus, little is known about the effect of these variables on the evolution and kinetics of granule formation in the TSG and the resulting granule structure. In a recent study, granule size distribution (GSD) evolution along the TSG screw was experimentally mapped in order to understand the dominant constitutive mechanisms of a granulation system such as growth, aggregation and breakage (Kumar et al., 2014a). However, such measurements provide a semi-quantitative insight regarding the GSD at discrete time steps, making it difficult to apply in process design applications. Population balance equations (PBEs) are a frequently used mathematical tool to describe particulate processes such as granulation (Kumar et al., 2013). An extensive review of the applications of such equations to particulate systems in engineering is given by Ramkrishna (2000). Butruso et al. (2014) used a multi-component population balance model (PBM) for tracking the liquid content and porosity of each particle size class during the twin-screw granulation. The experimental data from El Hagrasy et al. (2013) used for the study originated from samples collected from the granulator outlet and therefore a lumped-parameter approach was adopted for the development of the model.

In this study, the principle constitutive mechanisms of a granulation system such as growth, aggregation and breakage are included in a population balance modelling framework to track particle size evolution in the different individual screw blocks of a continuous TSG. Based on an experimentally determined inflow GSD (Kumar et al., 2014a) and mean residence time ( $\bar{t}$ ) (Kumar et al., 2014b) of the granulator, predictions of the outflow GSD were made. The experimental data was used for calibrating the model for individual screw modules in the TSG.

## 2. System analysis and model formulation

### 2.1. Continuous wet-granulation using TSG

The TSG consists of a barrel enclosing two co-rotating self-wiping screws. At the entrance, raw materials are fed into the transport zone and the granulation liquid is added via two nozzles, one for each screw, before the material reaches the mixing zone which consists of kneading discs (Fig. 1). The powder is hence wetted by the granulation liquid in this region. Further down, since the granulation occurs by a combination of capillary and viscous forces binding particles in the wet state, the wetted material is distributed, compacted and elongated by the kneading discs in the mixing zones, changing the particle morphology from small (microstructure) to large (macrostructure) (Vercruysse et al., 2012). The rotation of the screws conveys the material in axial direction through the different zones of the TSG by the drag and flow-induced displacement forces and thus causing mixing and granulation. The rheological behaviour of the material also changes based on liquid-to-solid ratio (L/S) (Althaus and Windhab, 2012).

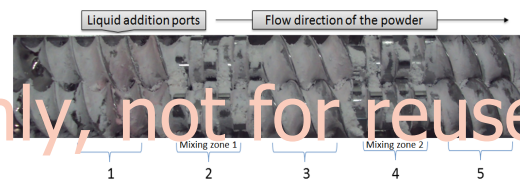


Figure 1: TSG screws with two mixing zones, each containing six kneading discs. Numbers indicate experimental sampling locations used for model calibration and validation.

## 2.2. Population balance model for twin-screw granulator

A TSG consists of a wetting zone and several mixing zones containing a finite number of kneading elements, which significantly drive the granulation process. The compartmentalisation into two mixing zones for simulation solved the challenge of inhomogeneous distribution in particle properties along the TSG length, due to the geometry of the screw as well as position of the liquid addition port. Introducing an external coordinate can be another possibility to model this inhomogeneity, but that will require implementation of the discrete element method together with population balances which is computationally challenging. In order to model the change in GSD across the individual mixing zone, these mixing zones were assumed as well-mixed systems. The granulation rate processes which are considered dominant in the kneading element regions of the granulator, i.e. aggregation and breakage, were included in a population balance modelling framework, which can be represented as:

$$\frac{\partial n(t, x)}{\partial t} = \frac{Q_{in}}{V} n_{in}(x) - \frac{Q_{out}}{V} n_{out}(x) + \frac{1}{2} \int_0^x \beta(t, x - \varepsilon, \varepsilon) n(t, x - \varepsilon) n(t, \varepsilon) d\varepsilon - n(t, x) \int_0^\infty \beta(t, x, \varepsilon) n(t, \varepsilon) d\varepsilon - \int_0^\infty b(x, \varepsilon) S(\varepsilon) n(t, \varepsilon) d\varepsilon - S(x) n(t, x) \quad (1)$$

where,  $n(t, x)$  is the number density function of particle volume as the internal co-ordinate at time  $t$ ,  $Q_{in}$  and  $Q_{out}$  were inflow and outflow of the material based on throughput and  $V$  was the volume of the mixing zone. Assuming the material transport across the mixing zone to occur at a steady state, inflow and outflow can be eliminated from Eq. 1. The primary challenge for using PBE is to model the kinetics of the twin-screw granulation process in  $\beta(t, x, \varepsilon)$  and  $b(x, \varepsilon)$ , because of their strong dependence on the time and in a fairly complex way on operating parameters and material properties. The constant aggregation kernel ( $\beta(t, x, \varepsilon) = 1$ ) describing the frequency that particles with diameter  $\varepsilon$  and  $x - \varepsilon$  collide to form a particle of size  $x$  was used in this study. For the breakage process, the quadratic selection function,  $S(y) = S_0(y)^\mu$ , where  $S_0$  and  $\mu$  are positive constants for reasons of simplicity. The breakage function,  $b(x, y)$  proposed by Austin (2002) (eq. 2) describing the formation of particles of size  $x$  from the breakup of a particle of size  $y$  was used.

$$b(x, y) = \frac{\phi \gamma x^{\gamma-1} + (1-\phi) \alpha x^{\alpha-1}}{\frac{\phi}{\gamma+1} + \frac{(1-\phi)}{\alpha+1}} \quad (2)$$

where  $\gamma$ ,  $\phi$  and  $\alpha$  are dimensionless material constants. The term  $\phi$  is called the weight parameter to quantify the mass content of the first breakage distributions. The exponents  $\gamma$  and  $\alpha$  represent the width of the fragment distributions  $\phi$  and  $1 - \phi$ , respectively.

## 2.3. Numerical solution of PBM

To solve this equation numerically we first fix a computational domain  $[0, R]$  with  $R < \infty$  and the truncated equation is obtained from Eq. 1 replacing 1 by  $R$ . A logarithmic grid with 50 bins was used for the discretisation of internal coordinates in order to accommodate particles of a wide size range with a minimal number of bins. Thereafter, a sectional method known as the cell average technique (CAT) was applied to solve the equation (Kumar et al., 2006). As the volumes of the newborn particles due to aggregation and/or breakage may lie between the bins of the logarithmic grid, the CAT allocates these particles into the corresponding nodes.

## 2.4. Model parameter estimation

The experimental data provided evidence that the aggregation and breakage are the dominant mechanisms in twin-screw granulation (for details see Kumar et al. (2014a)) and a model framework was developed to include these phenomena. However, various parameters in this model are

Table 1: Estimated model parameters with corresponding confidence intervals (95.44 %) at different screw speeds and mixing zones

Screw speed	Low		High	
Mixing zone	I	II	I	II
$\beta_0$	$3.02\text{E-}03 \pm 1.47\text{E-}04$	$1.95\text{E-}01 \pm 4.56\text{E-}02$	$9.18\text{E-}02 \pm 4.07\text{E-}03$	$4.99\text{E-}02 \pm 1.80\text{E-}02$
$S_0$	$2.53\text{E-}02 \pm 5.91\text{E-}03$	$7.99\text{E-}01 \pm 4.35\text{E-}02$	$3.11\text{E-}02 \pm 2.25\text{E-}03$	$5.72\text{E-}01 \pm 3.55\text{E-}02$
$\alpha$	$1.13\text{E-}05 \pm 8.83\text{E-}06$	$6.11\text{E-}01 \pm 3.19\text{E-}02$	$1.26\text{E-}03 \pm 3.29\text{E-}04$	$4.38\text{E-}01 \pm 9.30\text{E-}02$
$\gamma$	$4.05\text{E+}00 \pm 7.60\text{E-}01$	$3.81\text{E-}03 \pm 2.18\text{E-}04$	$2.63\text{E-}01 \pm 9.02\text{E-}03$	$4.49\text{E-}02 \pm 3.78\text{E-}03$
$\phi$	$1.03\text{E+}00 \pm 2.31\text{E-}01$	$5.43\text{E-}02 \pm 2.24\text{E-}03$	$1.18\text{E+}00 \pm 3.89\text{E-}01$	$1.50\text{E-}02 \pm 2.13\text{E-}03$

unknown and can vary based on process settings and material properties. Experimental data of volume distributions of granule samples from various locations inside the granulator (Fig. 1) were used to estimate values of five parameters: three dimensionless material constants,  $\gamma$ ,  $\phi$  and  $\alpha$  and the aggregation constant  $\beta_0$  and selection function constants  $S_0$ . Based on available literature, selection function constants  $\mu$  was fixed at 0.33. The estimation of these parameters was done by minimising the RMSE as an objective function (eq. 3):

$$\text{RMSE} = \sqrt{\frac{\sum_{i=1}^n (\hat{y}_i - y_i)^2}{n}} \quad (3)$$

where  $\hat{y}_i$  and  $y_i$  are the predicted and experimentally measured values for  $n$  bins of the granule size range. In order to find the global minimum of the objective function, the brute force method was used, which computed the objective function's value at each point of a multidimensional grid of points, to arrive at the global minimum of the function. This multidimensional grid contained ranges of  $\beta_0$  ( $1\text{e-}5$ ,  $0.4$ ),  $S_0$  ( $0.001$ ,  $3.5$ ),  $\alpha$  ( $3.3\text{e-}6$ ,  $1$ ),  $\gamma$  ( $1.6\text{e-}4$ ,  $5$ ) and  $\phi$  ( $0.01$ ,  $1.5$ ) with linear step length of  $0.005$ ,  $0.005$ ,  $0.00005$ ,  $0.5$  and  $0.5$ , respectively. The estimated parameter sets were useful to check any correlations between estimated parameters, and also to determine the confidence interval of the fitted parameter using the bootstrap estimation Efron and Tibshirani (1986). Later, to obtain a more precise (local) minimum, the downhill simplex algorithm was used applying the estimation result of brute force minimization as initial guess (Nelder and Mead, 1965). The implementation of PBM solution and parameter estimates were performed using the Python programming language, employing built-in functions in scientific libraries NumPy and SciPy (Oliphant, 2007) and Quespy (Langtangen and Wang, 2014).

### 3. Results and discussion

#### 3.1. Parameter estimation for predictive modelling

Experimentally measured size distributions from location 1, 3 and 5 in Fig. 1 for runs at low (500 rpm) and high (900 rpm) screw speed were used for model calibration. In order to quantitatively represent these trends in the simulations, the unknown rate parameters of the aggregation and Austin breakage kernels were estimated by comparing the simulation results with experimental data. The estimated parameters used for the numerical computations and their confidence intervals (95.44 %) are listed in table 1. The error estimates (RMSE and  $R^2$ ) are mentioned in Fig. 2. The low RMSE and high  $R^2$  values for all the screw speeds and mixing zones indicate that numerical results were in excellent agreement with the experimental data for each location inside the granulator subject to different optimal model parameters.

#### 3.2. Simulated dynamic behaviour in the mixing zones of TSG

The simulation results showed that when the screw speed is low (Fig. 2.a), the  $D_{90}$  and  $D_{75}$  reduced and the  $D_{25}$  and  $D_{50}$  increased slightly when the material passed the first mixing zone. This indicates that the primary role of the first kneading block at this condition was the breaking of larger wetted lumps. The granules resulting from breakage caused increase in  $D_{25}$  and  $D_{50}$ . The

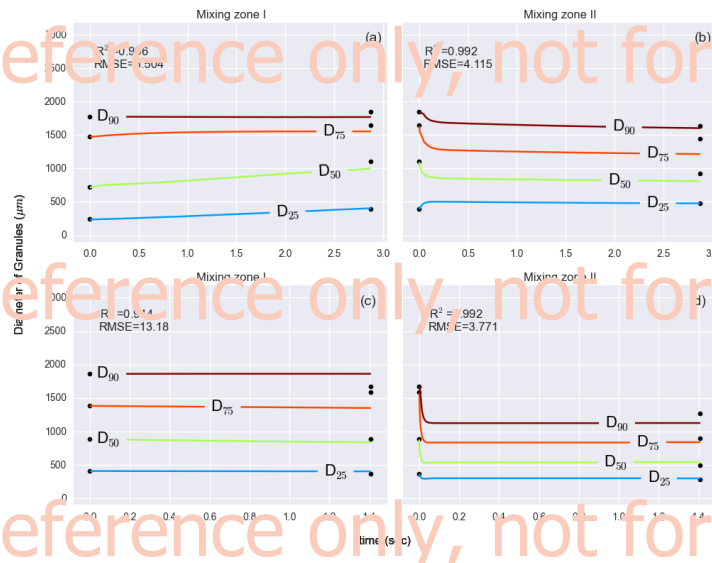


Figure 2: Experimental (●) and simulated (—) trends for dynamic change in quartiles of GSD (D25, D50, D75 and D90) at low (a and b) and high (c and d) screw speeds for first (a and c) and second (b and d) mixing zones.

second mixing zone at this condition caused further breakage of the granules leading to reduction in  $D_{50}$  as well together with  $D_{75}$  and  $D_{90}$  (Fig. 2.c). However, the  $D_{25}$  of the GSD remained unaffected by the mixing in the second zone. Overall, the barrel at this condition was highly filled due to the low screw conveying rate at low screw speed leading to less space for material to get distributed. This was also the reason that in experimental study this condition led to an undesirable level of high torque Kumar et al. (2014a).

The simulation of the high screw speed condition showed a significant change in the granulation behaviour in two mixing zones (Fig. 2.c and d). Unlike low screw speed where the material passed through the first mixing zone at this condition all the quartiles of the GSD increased (Fig. 2.c). This indicates that aggregation was the most dominant mechanism in this condition in this mixing zone, while the level of breakage was very low leading to no reduction in any fraction with time. However, when the material was introduced to the second kneading block, the quartile values  $D_{90}$ ,  $D_{75}$ ,  $D_{50}$  dropped significantly, which indicates that breakage returned as the dominant mechanism in the second mixing zone (Fig. 2.d). This observation by process simulation is very important as it established that the successive kneading block led to a granulation regime separation inside the twin-screw granulator under this condition. The mixing of the wetted powder in the first kneading block caused an increase in the aggregation rate, which was reduced after the second kneading block. However, the breakage rate increased successively along the length of the granulator. Such a physical separation between the granulation regimes will be promising for future design and advanced control of the continuous granulation process.

In order to further improve the model, future work will focus on introducing the wetting kinetics in the model framework and to obtain particle flux data and collision frequencies using DEM to avoid the parameter estimation by model inversion. Additionally, dedicated mechanistic kernels for the twin-screw granulation can be developed in order to improve the sensitivity of the model towards the change in process condition and other field parameters. Finally, a validated model can be used to define the design space of the process for the future optimization and model-based control of the granulation process.



#### 4. Conclusions

A 1-D PBIM including aggregation and breakage sub-processes for a continuous twin-screw granulation process was presented. Unknown model parameters and their 95% confidence range were estimated using experimentally measured particle size distributions from inside the granulator. The calibrated model was then used as a predictive tool within the experimental space. The results showed strong agreement with experimental data. This approach is the better way forward for the development of twin-screw granulation models as multiple factors of twin-screw granulator leading to a experimental output can now constrain the model during calibration. Further analysis revealed that, at a high screw speed, the successive kneading blocks can lead to the occurrence of different constitutive granulation mechanisms inside the twin-screw granulator. An ability to achieve a physical separation between the granulation regimes inside the granulator can be promising for future design and advanced control of the continuous granulation process using the twin-screw granulator. Furthermore, the study suggested that a model-based approach can be adopted to develop a better understanding of twin-screw granulation processes. A validated model can ultimately be used to define the design space of the process to facilitate process optimization and model-based control.

#### Acknowledgements

Financial support for this research from the BOF (Bijzonder Onderzoeksfonds Universiteit Gent, Research Fund Ghent University) is gratefully acknowledged.

#### References

- Albano, T. C., Winkler, F. J., Jan, 2012. Characterization of wet powder flowability by shear cell measurements and compaction curves. *Powder Technol.* 215–216, 59–63.
- Austin, L. G., 2002. A treatment of impact breakage of particles. *Powder Technol.* 126 (1), 85–90.
- Barrasso, D., Hagrasy, A. E., Litster, J. D., Ramachandran, R., 2014. Multi-dimensional population balance model development and validation for a twin screw granulation process. *Powder Technol.*
- Dhenge, R. M., Cartwright, J. J., Doughty, D. G., Hounslow, M. J., Salman, A. D., 2011. Twin screw wet granulation: Effect of powder feed rate. *Adv. Powder Technol.* 22 (2), 162–166.
- Dhenge, R. M., Washino, K., Cartwright, J. J., Hounslow, M. J., Salman, A. D., 2013. Twin screw granulation using conveying screws: Effects of viscosity of granulation liquids and flow of powders. *Powder Technol.* 238, 77–90.
- Fienberg, B., Tibshirani, R., 1996. Bootstrapping methods for standard errors, confidence intervals, and other measures of statistical accuracy. *Statistical Science* 1 (1), pp. 54–75.
- El Hagrasy, A., Hennenkamp, J., Burke, M., Cartwright, J., Litster, J., 2013. Twin screw wet granulation: Influence of formulation parameters on granule properties and growth behavior. *Powder Technol.* 238, 108–115.
- Kumar, A., Gernaey, K. V., De Beer, T., Nopens, I., 2013. Model-based analysis of high shear wet granulation from batch to continuous processes in pharmaceutical production – a critical review. *Eur. J. Pharm. Biopharm.* 85 (3, Part B), 814–832.
- Kumar, A., Vercruyse, J., Bellandi, G., Gernaey, K. V., Vervaet, C., Remon, J. P., Beer, T. D., Nopens, I., 2014a. Experimental investigation of granule size and shape dynamics in twin-screw granulation. *International Journal of Pharmaceutics* 475 (1–2), 433–445.
- Kumar, A., Vercruyse, J., Toivainen, M., Panouliot, P.-E., Jutila, M., Vanhoorne, V., Vervaet, C., Remon, J. P., Gernaey, K. V., Beer, T. D., et al., 2014b. Mixing and transport during pharmaceutical twin-screw wet granulation: experimental analysis via chemical imaging. *Eur. J. Pharm. Biopharm.*
- Kumar, J., Peglow, M., Warnecke, G., Heinrich, S., Morl, L., 2006. Improved accuracy and convergence of discretized population balance for aggregation: The cell average technique. *Chem. Eng. Sci.* 61 (10), 3327–3342.
- Langtangen, H. P., Wang, L., 2014. Odespy software package. <https://github.com/hplgit/odespy>.
- Nelder, J. A., Mead, R., 1965. A simplex method for function minimization. *Comput. J.* 7 (4), 308–313.
- Oliphant, T. E., 2007. Python for scientific computing. *Comput. Sci. Eng.* 9 (3), 10–20.
- Parthasarathy, L., 2000. Population balance: Theory and applications to particulate systems in engineering. Academic press.
- Thompson, M. R., Sun, J., 2010. Wet granulation in a twin-screw extruder: Implications of screw design. *J. Pharm. Sci.* 99 (4), 2090–2103.
- Vercruyse, J., Córdoba Díaz, D., Peeters, E., Fonteyne, M., Delaet, U., Van Assche, I., De Beer, T., Remon, J. P., Vervaet, C., 2012. Continuous twin screw granulation: Influence of process variables on granule and tablet quality. *Eur. J. Pharm. Biopharm.* 82 (1), 205–211.